Supporting Information

The Swi/Snf chromatin remodeling/tumor suppressor complex establishes nucleosome occupancy at target promoters

Michael Y. Tolstorukov[1], Courtney G. Sansam[1], Ping Lu[1], Edward C. Koellhoffer, Katherine C. Helming, Burak H. Alver, Erik J. Tillman, Julia A. Evans, Boris G. Wilson, Peter J. Park[2], Charles W.M. Roberts[2]

[1]equal contribution; [2]co-corresponding authors

Additional validation of the main observations

Decrease in nucleosome occupancy in peri-TSS regions in the mutant samples (Fig. 1 in Main text) could, in principle, be an artifact of the difference in experimental conditions, such as difference in the concentration of MNase used for chromatin fragmentation [Weiner et al., 2010], or data processing. To address this issue, we repeated the nucleosome profiling experiments in tightly controlled setting using paired-end sequencing strategy and two independent MNase concentrations, corresponding to light and moderate digestion conditions. We used Illumina sequencing in this case to address possible platform bias at the same time.

Since we used paired-end sequencing, we could directly investigate the distribution mono-nucleosome fragment sizes in each sample. The average fragment size bears information about the level of digestion [Johnson et al., 2006], with the values smaller than 145-147-bp generally indicating 'over-digestion' and the values larger than 147-150 bp indicating 'under-digestion'. The fragment size distributions for each sample are shown in Fig. S4*A,B*. The distributions are remarkably similar for each MNase concentration, indicating a high level of similarity in the depths of digestion for mutant and wild type samples. In the case of light digestion, the average fragment size is 167-169 bp, which suggests that linker DNA was not completely removed from the mono-nucleosomes in this case. The relatively narrow distribution with the average size of

146-147 bp in the case of moderate digestion conditions indicates that most of the sequenced fragments correspond to full-length mono-nucleosomes free of linker DNA.

We next compared the average nucleosome frequency profiles at peri-TSS regions in the wild type and mutant samples for both digestion conditions (Fig. S4*C,D*). The nucleosome occupancy profiles were similar for all samples in the case of the light digestion (Fig. S4*C*). This observation strongly argues against the possibility that mutant samples have a systematic difference from the wild type, which would preclude reaching the same level of chromatin fragmentation under similar digestion conditions. At the moderate level of digestion (Fig. S4*D*) the nucleosome occupancy in the mutant cells was lower than in the wild type in the region of about +/-1 Kb around TSS, in line with our results for the Helicos data (main Fig.1). Furthermore, the comparison of average nucleosome occupancy within genes, which represent larger genomic regions than peri-TSS regions, shows that the estimates based on the Illumina data correlate well with the Helicos estimates (Fig. S4*E*). Thus, the similar results obtained on the Illumina and Helicos data validate our findings.

Supporting Methods

Data Analysis. ***Sequence read alignment and preprocessing.*** For the main data sets used in this study sequencing was performed on the HeliScope, a single-molecule sequencer from Helicos Biosciences Corporation. Low-quality sequenced tags were removed and the remaining tags were mapped to the mouse genome (mm9) using the manufacturer's software suite with default parameters. The Illumina sequencing platform was used to produce additional nucleosomal data for the samples digested under higher and lower MNase concentrations. These data sets were mapped to the mouse genome using Bowtie aligner [Langmead et al., 2009]. For all data sets, genomic positions with anomalously high counts of mapped tags

(above a *Z*-score of 7) were noted and tags mapped to such positions were discarded. The final read counts for the nucleosomal and Brg1 data sets are provided in Table S3.

***Calculation of average profiles*.** Tag counts were scaled to account for differences in absolute tag counts between samples. Data were normalized to represent occurrences per one million aligned reads in the promoter regions of each sample. The positions of single-end sequenced tags correspond to the 5'-ends of the mononucleosomal fragments; therefore these positions were shifted by half of the characteristic fragment size (75 bp) towards their 3'-ends to represent centers of the DNA fragments. The positions from positive and negative DNA strands were combined and the resulting tag frequency profiles were smoothed in a 75-bp running window. Average profiles obtained for the individual gene clusters (Fig. S2*B*) were additionally normalized so that the baseline nucleosome occupancy at regions -700..-600 bp is similar for all cell types within each cluster to focus on the profile differences in close proximity to gene starts. The profiles of the Brg1 ChIP tag density around transcription start sites were normalized by subtracting the tag density obtained from sequencing of the input DNA sample.

Relative nucleosome occupancy score. The score was computed for each gene by adding the nucleosome tag counts at -1 and +1 nucleosome sites (positions from -300 to -150 and from 50 to 200 relative to TSS), subtracting the tag count at NDR (positions from -100 to 0), and normalizing the resulting score by the 'baseline' tag count (positions from +/-2kb to +/-1 kb). To avoid possible artifacts due to low tag coverage in some genomic regions, only the genes with non-zero tag counts at -1 and +1 nucleosome positions and non-zero baseline tag counts were used (14,247 genes).

Expression analysis. Gene expression data were generated on GeneChip Mouse Genome 430A 2.0 Arrays (Affymetrix) and processed using the bioconductor package Affy (http://www.bioconductor.org). Different background correction and normalization methods were explored to ensure robustness of our results and the MAS 5.0 algorithm was used for the final

analysis. Expressed and silent genes in the analysis of average nucleosome profiles and nucleosome occupancy scores were identified using the MAS 5.0 present/absent calls for the WT sample. P-values for gene expression changes were calculated based on the replicates of each sample (t-test). Differentially expressed genes were identified as those with absolute value of log2 of expression fold-change above 0.5, p-value below 0.05, and magnitudes of expression in the top 75% of all tested genes (Fig. S6).

***Gene Ontology analysis*.** Gene ontology analysis was performed using the Gene Ontology Term Finder (Boyle et al., 2004; http://go.princeton.edu/cgi-bin/GOTermFinder/GOTermFinder). The P-values were corrected for multiple hypotheses using the algorithm implemented on the web-server.

References

Weiner A, Hughes A, Yassour M, Rando OJ, Friedman N (2010) High-resolution nucleosome mapping reveals transcription-dependent promoter packaging. Genome Res 20: 90-100.

Johnson SM, Tan FJ, McCullough HL, Riordan DP, Fire AZ (2006) Flexibility and constraint in the nucleosome core landscape of Caenorhabditis elegans chromatin. Genome Res 16:1505-1516.

Langmead B, Trapnell C, Pop M, & Salzberg SL (2009) Ultrafast and memory-efficient alignment of short DNA sequences to the human genome. Genome Biol., 10:R25

Boyle EI, Weng S, Gollub J, Jin H, Botstein D, Cherry JM, & Sherlock G (2004) GO::TermFinder--open source software for accessing Gene Ontology information and finding significantly enriched Gene Ontology terms associated with a list of genes. Bioinformatics. 20:3710-3715.

Table S1. Groups of the genes with low and high enrichment in Brg1

	Brg1 Low Count	% of All	Brg1 High Count	% of All
All	4757	100	8100	100
CpGi	955	20.08	6106	75.38
Non-CpGi	3802	79.92	1994	24.62
All-Expressed	866	18.2	4738	58.49
All-Silent	3341	70.23	1499	18.51
CpGi-Expressed	261	5.49	3722	45.95
CpGi-Silent	550	11.56	934	11.53
Non-CpGi-Expressed	605	12.72	1016	12.54
Non-CpGi-Silent	2791	58.67	565	6.98

Table S2. Gene ontology analysis for up- and down-regulated genes in mutant cells

Up-regulated upon Snf5 depletion (P < 0.01)

Gene Ontology term	Cluster frequency	Genome frequency	Enrichment (cluster freq/genome freq)	Corrected P-value
cell cycle process	68 of 830 genes, 8.2%	555 of 12832 genes, 4.3%	1.91	0.00047
cell cycle phase	54 of 830 genes, 6.5%	408 of 12832 genes, 3.2%	2.03	0.00078
mitotic cell cycle	54 of 830 genes, 6.5%	410 of 12832 genes, 3.2%	2.03	0.00092
cell division	42 of 830 genes, 5.1%	298 of 12832 genes, 2.3%	2.22	0.00315

Down-regulated upon Snf5 depletion (P < 0.01): None

Up-regulated upon Brg1 depletion (P < 0.01)

Gene Ontology term	Cluster frequency	Genome frequency	Enrichment (cluster freq/genome freq)	Corrected P-value
DNA metabolic process	117 of 1258 genes, 9.3%	440 of 12832 genes, 3.4%	2.74	1.76E-21
cell cycle	169 of 1258 genes, 13.4%	790 of 12832 genes, 6.2%	2.16	1.52E-20
cell cycle process	133 of 1258 genes, 10.6%	555 of 12832 genes, 4.3%	2.47	3.64E-20
cell cycle phase	107 of 1258 genes, 8.5%	408 of 12832 genes, 3.2%	2.66	6.79E-19
M phase	88 of 1258 genes, 7.0%	303 of 12832 genes, 2.4%	2.92	2.76E-18
nucleic acid metabolic process	376 of 1258 genes, 29.9%	2509 of 12832 genes, 19.6%	1.53	2.36E-17
response to DNA damage stimulus	86 of 1258 genes, 6.8%	315 of 12832 genes, 2.5%	2.72	6.74E-16
mitotic cell cycle	101 of 1258 genes, 8.0%	410 of 12832 genes, 3.2%	2.50	1.46E-15
chromosome segregation	39 of 1258 genes, 3.1%	81 of 12832 genes, 0.6%	5.17	2.29E-15
nucleobase, nucleoside, nucleotide and nucleic acid metabolic process	423 of 1258 genes, 33.6%	2999 of 12832 genes, 23.4%	1.44	3.61E-15
M phase of mitotic cell cycle	67 of 1258 genes, 5.3%	217 of 12832 genes, 1.7%	3.12	6.65E-15
DNA replication	58 of 1258 genes, 4.6%	177 of 12832 genes, 1.4%	3.29	6.00E-14
mitosis	64 of 1258 genes, 5.1%	210 of 12832 genes, 1.6%	3.19	8.05E-14
cell division	79 of 1258 genes, 6.3%	298 of 12832 genes, 2.3%	2.74	1.33E-13
organelle fission	65 of 1258 genes, 5.2%	220 of 12832 genes, 1.7%	3.06	2.57E-13
DNA repair	66 of 1258 genes, 5.2%	230 of 12832 genes, 1.8%	2.89	7.56E-13
cellular nitrogen compound metabolic process	437 of 1258 genes, 34.7%	3220 of 12832 genes, 25.1%	1.38	1.05E-12
chromosome organization	87 of 1258 genes, 6.9%	364 of 12832 genes, 2.8%	2.46	3.23E-12

nitrogen compound metabolic process	440 of 1258 genes, 35.0%	3306 of 12832 genes, 25.8%	1.36	2.69E-11
organelle organization	188 of 1258 genes, 14.9%	1136 of 12832 genes, 8.9%	1.67	1.56E-10
DNA conformation change	31 of 1258 genes, 2.5%	82 of 12832 genes, 0.6%	4.17	2.58E-08
cellular component organization at cellular level	220 of 1258 genes, 17.5%	1469 of 12832 genes, 11.4%	1.54	3.17E-08
cellular macromolecule metabolic process	499 of 1258 genes, 39.7%	4016 of 12832 genes, 31.3%	1.27	4.40E-08
cellular response to stress	105 of 1258 genes, 8.3%	559 of 12832 genes, 4.4%	1.89	6.41E-08
cellular component organization or biogenesis at cellular level	228 of 1258 genes, 18.1%	1549 of 12832 genes, 12.1%	1.50	7.04E-08
regulation of nucleobase, nucleoside, nucleotide and nucleic acid metabolic process	278 of 1258 genes, 22.1%	2058 of 12832 genes, 16.0%	1.38	4.15E-06
DNA-dependent DNA replication	20 of 1258 genes, 1.6%	47 of 12832 genes, 0.4%	4.00	1.10E-05
regulation of nitrogen compound metabolic process	278 of 1258 genes, 22.1%	2078 of 12832 genes, 16.2%	1.36	1.13E-05
regulation of cell cycle	72 of 1258 genes, 5.7%	366 of 12832 genes, 2.9%	1.97	1.32E-05
microtubule cytoskeleton organization	36 of 1258 genes, 2.9%	130 of 12832 genes, 1.0%	2.90	1.33E-05
DNA packaging	23 of 1258 genes, 1.8%	62 of 12832 genes, 0.5%	3.60	1.88E-05
DNA recombination	30 of 1258 genes, 2.4%	99 of 12832 genes, 0.8%	3.00	2.60E-05
regulation of macromolecule metabolic process	315 of 1258 genes, 25.0%	2436 of 12832 genes, 19.0%	1.32	3.10E-05
cellular macromolecule biosynthetic process	316 of 1258 genes, 25.1%	2448 of 12832 genes, 19.1%	1.31	3.52E-05
regulation of cellular macromolecule biosynthetic process	259 of 1258 genes, 20.6%	1932 of 12832 genes, 15.1%	1.36	3.82E-05
cellular response to stimulus	139 of 1258 genes, 11.0%	900 of 12832 genes, 7.0%	1.57	4.97E-05
nucleotide-excision repair, DNA gap filling	11 of 1258 genes, 0.9%	16 of 12832 genes, 0.1%	9.00	5.57E-05
chromatin organization	57 of 1258 genes, 4.5%	275 of 12832 genes, 2.1%	2.14	8.17E-05
macromolecule metabolic process	526 of 1258 genes, 41.8%	4473 of 12832 genes, 34.9%	1.20	8.73E-05
regulation of primary metabolic process	322 of 1258 genes, 25.6%	2529 of 12832 genes, 19.7%	1.30	0.0001
chromosome condensation	12 of 1258 genes, 1.0%	20 of 12832 genes, 0.2%	5.00	0.00011
transcription	245 of 1258 genes, 19.5%	1831 of 12832 genes, 14.3%	1.36	0.00012
cellular component organization	297 of 1258 genes, 23.6%	2307 of 12832 genes, 18.0%	1.31	0.00015
gene expression	335 of 1258 genes, 26.6%	2661 of 12832 genes, 20.7%	1.29	0.00017

cellular component organization or biogenesis	306 of 1258 genes, 24.3%	2395 of 12832 genes, 18.7%	1.30	0.00019
regulation of transcription	238 of 1258 genes, 18.9%	1777 of 12832 genes, 13.8%	1.37	0.00019
macromolecule biosynthetic process	318 of 1258 genes, 25.3%	2509 of 12832 genes, 19.6%	1.29	0.00021
regulation of macromolecule biosynthetic process	260 of 1258 genes, 20.7%	1982 of 12832 genes, 15.4%	1.34	0.00026
mitotic sister chromatid segregation	12 of 1258 genes, 1.0%	22 of 12832 genes, 0.2%	5.00	0.0005
microtubule-based process	43 of 1258 genes, 3.4%	193 of 12832 genes, 1.5%	2.27	0.0005
centrosome organization	14 of 1258 genes, 1.1%	30 of 12832 genes, 0.2%	5.50	0.00059
regulation of cellular metabolic process	334 of 1258 genes, 26.6%	2694 of 12832 genes, 21.0%	1.27	0.0009
sister chromatid segregation	12 of 1258 genes, 1.0%	23 of 12832 genes, 0.2%	5.00	0.00095
chromatin modification	49 of 1258 genes, 3.9%	242 of 12832 genes, 1.9%	2.05	0.00158
cellular metabolic process	610 of 1258 genes, 48.5%	5418 of 12832 genes, 42.2%	1.15	0.00284
regulation of gene expression	261 of 1258 genes, 20.7%	2049 of 12832 genes, 16.0%	1.29	0.00324
nucleotide-excision repair	17 of 1258 genes, 1.4%	48 of 12832 genes, 0.4%	3.50	0.00372
microtubule organizing center organization	14 of 1258 genes, 1.1%	34 of 12832 genes, 0.3%	3.67	0.00391
regulation of cellular biosynthetic process	265 of 1258 genes, 26.1%	2091 of 12832 genes, 16.3%	1.60	0.00401
regulation of cell cycle process	39 of 1258 genes, 3.1%	181 of 12832 genes, 1.4%	2.21	0.00449
primary metabolic process	612 of 1258 genes, 48.6%	5456 of 12832 genes, 42.5%	1.14	0.00476
regulation of metabolic process	364 of 1258 genes, 28.9%	3025 of 12832 genes, 23.6%	1.22	0.00503
regulation of biosynthetic process	267 of 1258 genes, 21.2%	2118 of 12832 genes, 16.5%	1.28	0.00563
negative regulation of cell cycle	40 of 1258 genes, 3.2%	190 of 12832 genes, 1.5%	2.13	0.00615
centrosome cycle	10 of 1258 genes, 0.8%	19 of 12832 genes, 0.1%	8.00	0.00843
RNA metabolic process	216 of 1258 genes, 17.2%	1662 of 12832 genes, 13.0%	1.32	0.00852
meiosis	24 of 1258 genes, 1.9%	90 of 12832 genes, 0.7%	2.71	0.00989

Down-regulated upon Brg1 depletion (P < 0.01)

Gene Ontology term	**Cluster frequency**	**Genome frequency**	**Enrichment** (cluster freq+D26/genome	**Corrected P-value**
locomotion	75 of 789 genes, 9.5%	615 of 12832 genes, 4.8%	1.98	1.51E-05
regulation of cell migration	38 of 789 genes, 4.8%	233 of 12832 genes, 1.8%	2.67	6.42E-05
regulation of cell motility	38 of 789 genes, 4.8%	235 of 12832 genes, 1.8%	2.67	8.13E-05
cell migration	59 of 789 genes, 7.5%	457 of 12832 genes, 3.6%	2.08	9.10E-05

enzyme linked receptor protein signalir	55 of 789 genes, 7.0%	421 of 12832 genes, 3.3%	2.12	0.00017
blood vessel morphogenesis	40 of 789 genes, 5.1%	267 of 12832 genes, 2.1%	2.43	0.0003
regulation of locomotion	39 of 789 genes, 4.9%	259 of 12832 genes, 2.0%	2.45	0.00038
cell motility	59 of 789 genes, 7.5%	481 of 12832 genes, 3.7%	2.03	0.00055
localization of cell	59 of 789 genes, 7.5%	481 of 12832 genes, 3.7%	2.03	0.00055
regulation of cell communication	85 of 789 genes, 10.8%	794 of 12832 genes, 6.2%	1.74	0.00058
regulation of cellular component move	38 of 789 genes, 4.8%	258 of 12832 genes, 2.0%	2.40	0.00097
response to chemical stimulus	119 of 789 genes, 15.1%	1253 of 12832 genes, 9.8%	1.54	0.00146
vasculature development	44 of 789 genes, 5.6%	327 of 12832 genes, 2.5%	2.24	0.00162
regulation of system process	43 of 789 genes, 5.4%	318 of 12832 genes, 2.5%	2.16	0.0019
regulation of biological quality	139 of 789 genes, 17.6%	1532 of 12832 genes, 11.9%	1.48	0.002
cellular component movement	60 of 789 genes, 7.6%	513 of 12832 genes, 4.0%	1.90	0.00223
cell adhesion	65 of 789 genes, 8.2%	578 of 12832 genes, 4.5%	1.82	0.00313
transmembrane receptor protein tyrosi	37 of 789 genes, 4.7%	262 of 12832 genes, 2.0%	2.35	0.00392
regulation of cell proliferation	79 of 789 genes, 10.0%	764 of 12832 genes, 6.0%	1.67	0.00631
blood vessel development	41 of 789 genes, 5.2%	315 of 12832 genes, 2.5%	2.08	0.00912

Table S3. Read counts in the data sets used in the study

	Wild type	Snf5$^{-/-}$	Brg1$^{-/-}$
Nucleosomal data sets			
Helicos[1]	79	66	37
Illumina, higher MNase[2]	33	20	38
Illumina, lower MNase[2]	8	49	33
Brg1 data sets			
ChIP[1]	14	-	-
Input[1]	6	-	-

The counts are provided in millions of aligned reads
[1]Single-end reads
[2]Paired-end reads

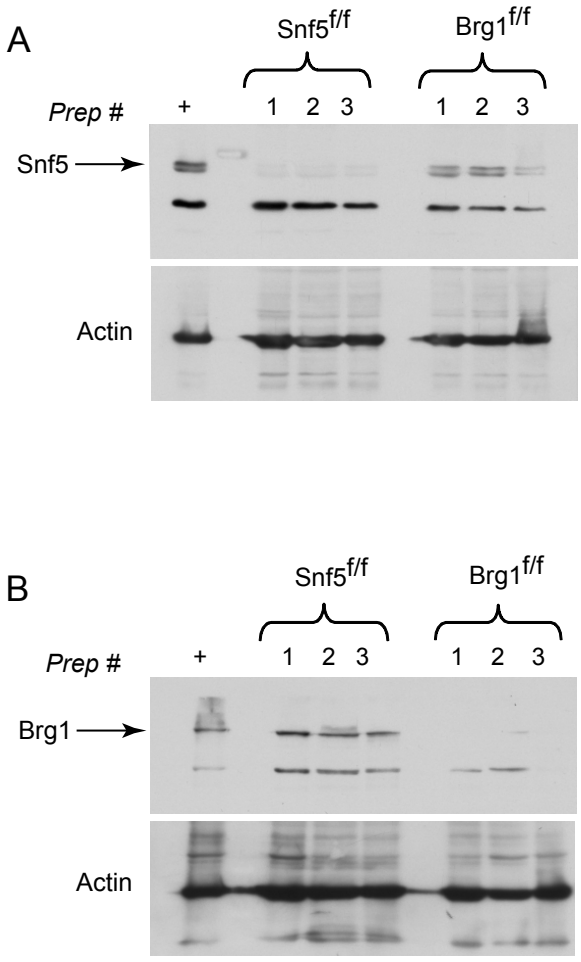

Figure S1. Snf5 and Brg1are efficiently deleted in conditional MEFs.
Primary WT, Snf5$^{f/f}$, and Brg1$^{f/f}$ MEFs were infected with a retrovirus containing Cre recombinase and selected in media containing puromycin. Deletion of Snf5 or Brg1 was confirmed by immunoblot for Snf5 *(A)* and Brg1 *(B)*. B-actin was used as a loading control. Three independent experiments are shown, numbered 1, 2, 3.

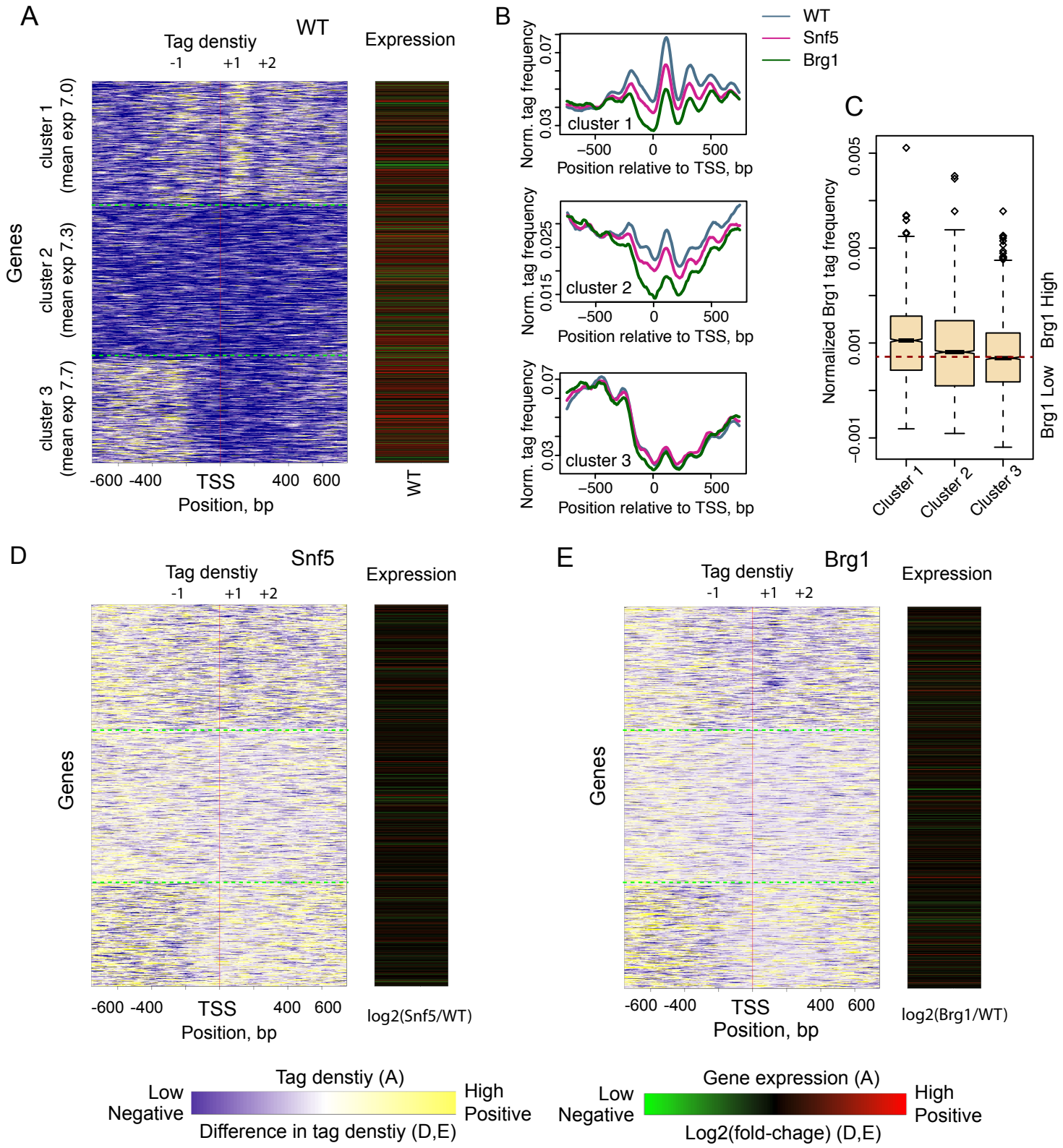

Figure S2. Diversity of nucleosomal profiles at the individual gene level. *(A)* Heat map on the left represents smoothed nucleosome tag frequencies at individual genes in WT. Expression level of each gene is shown on the right to tag density heat map. The genes were placed in three groups by K-means clustering of the tag density. The mean expression score (log2 scale) is given for each cluster. *(B)* Average nucleosomal profiles for genes comprising clusters 1-3. The profiles were normalized within each cluster (see Methods for detail). *(C)* Boxplot showing Brg1 prevalence at TSS of the genes from clusters 1-3. Dashed horizontal line gives a reference of the threshold used to define groups “Brg1 Low” and “Brg1 High” in Fig. 3 in the Main text. *(D)* Heat maps representing difference between nucleosome tag frequencies at individual genes in Snf5-deficient and WT samples (left) and fold-changes in expression levels (log2 scale, right). *(E)* The same as *(D)* for Brg1-deficient cells. The genes in *(D,E)* are placed in the same groups as genes in *(A)*, i.e. all clusters are based on WT data. We note that the expression levels vary within each group, indicating that none of the groups entirely corresponds to the ‘expressed’ or ‘silent’ genes.

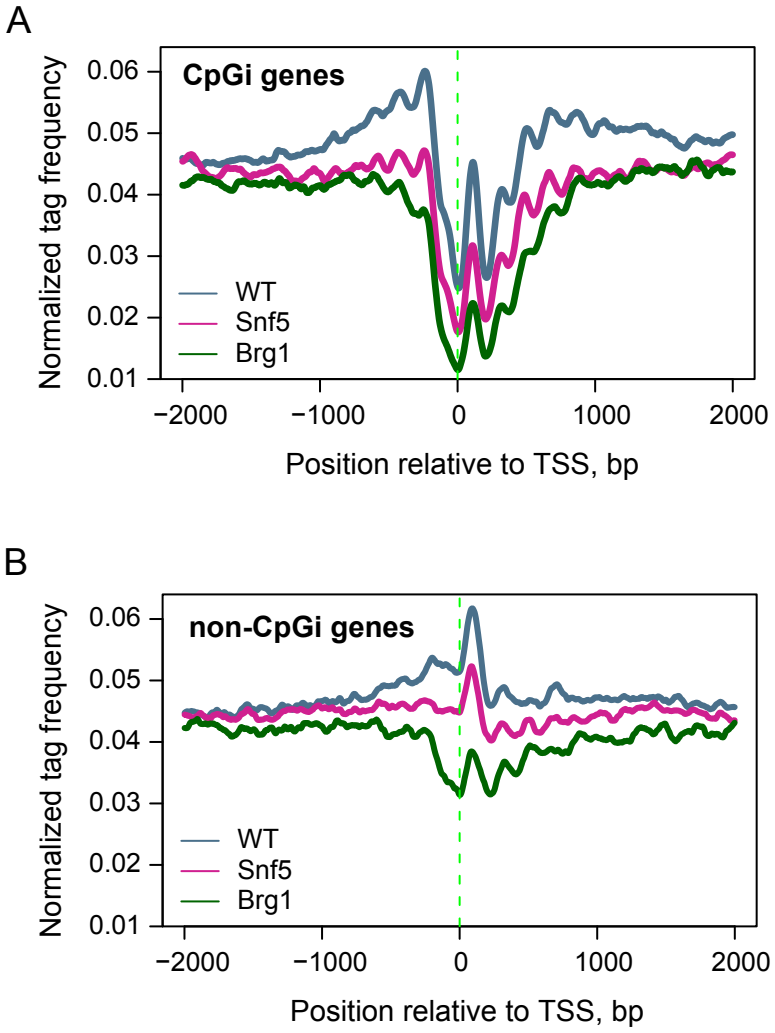

Figure S3. Genome-wide nucleosome occupancy profiles at peri-TSS regions for the genes associated (*A*) and not associated (*B*) with CpG islands at TSS.

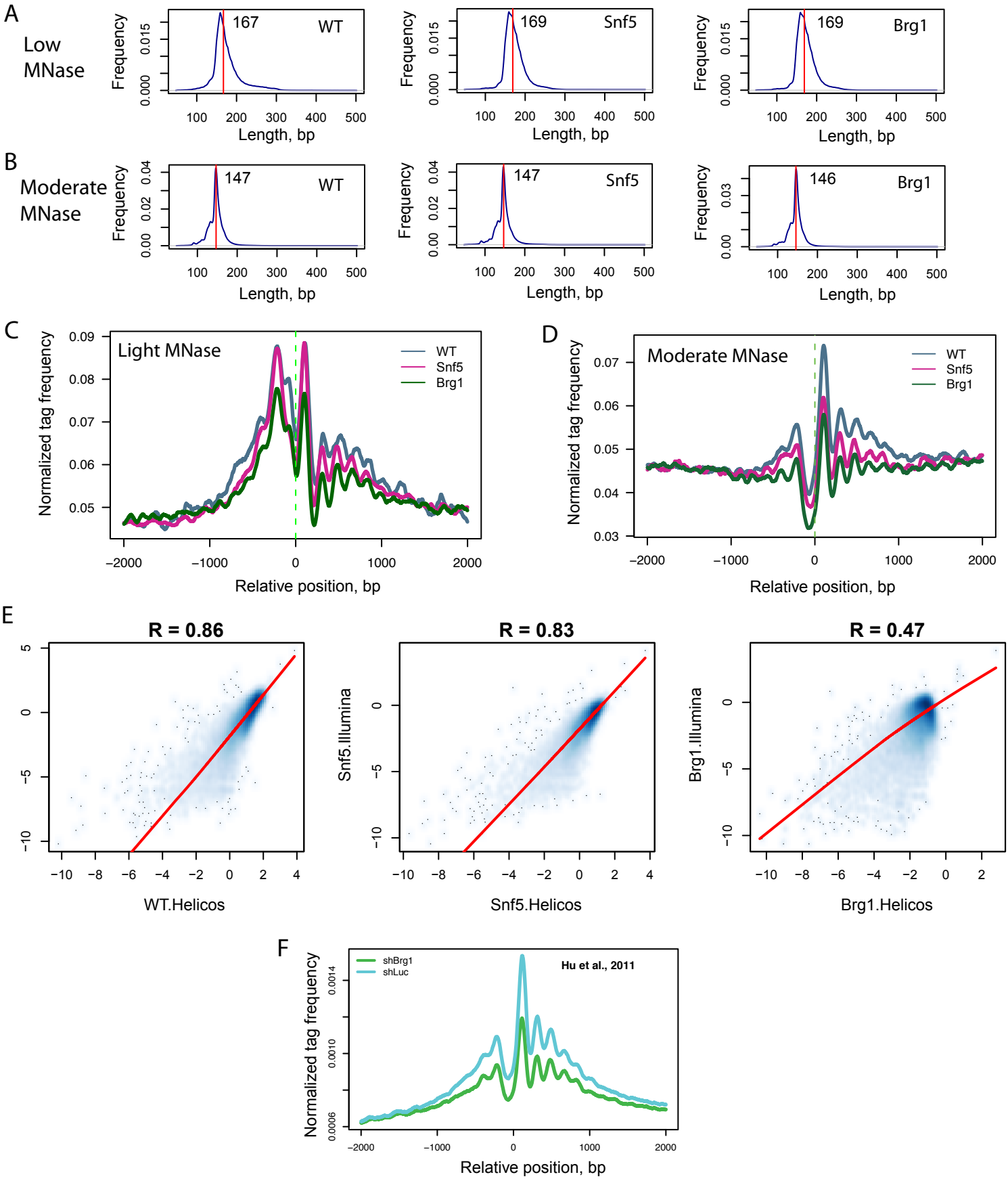

Figure S4. Nucleosome profiling with two MNase concentrations. *(A,B)* Distribution of the fragment lengths for each sample under the conditions of light *(A)* and moderate *(B)* digestion. *(C,D)* The normalized nucleosome frequency profiles for wild type and mutant samples corresponding to light *(C)* and moderate *(D)* digestion conditions. *(E)* Correlations between average nucleosome tag frequency in Illumina/Solexa (moderated digestion) and Helicos data computed for the regions corresponding to the annotated genes extended by 1 Kb on each side. *(F)* Nucleosme profiles for Brg1-depeleted and control samples based on the independent data (Hu et al., Genome Res 2011)

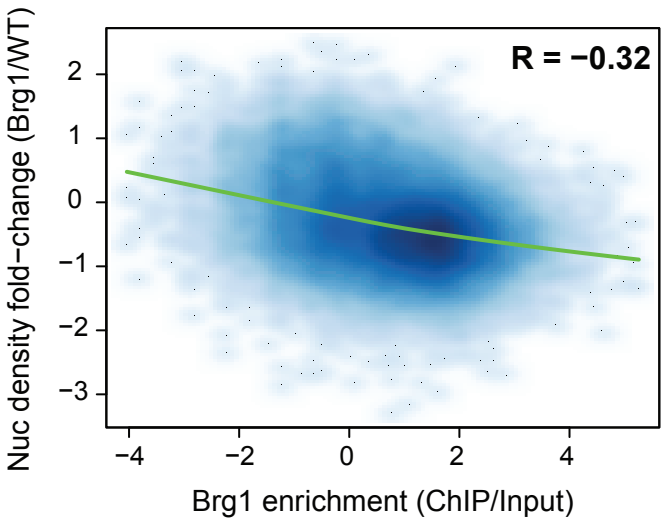

Figure S5. Brg1 enrichment compared to magnitude of nucleosome density changes upon Brg1 depletion. Each blue dot represents a gene. Brg1 enrichment and fold-change in nucleosome density upon Brg1 inactivation were computed (log2 scale) for the TSS regions (+/-2 kb). The Pearson correlation coefficient is indicated and a smooth regression line is shown.

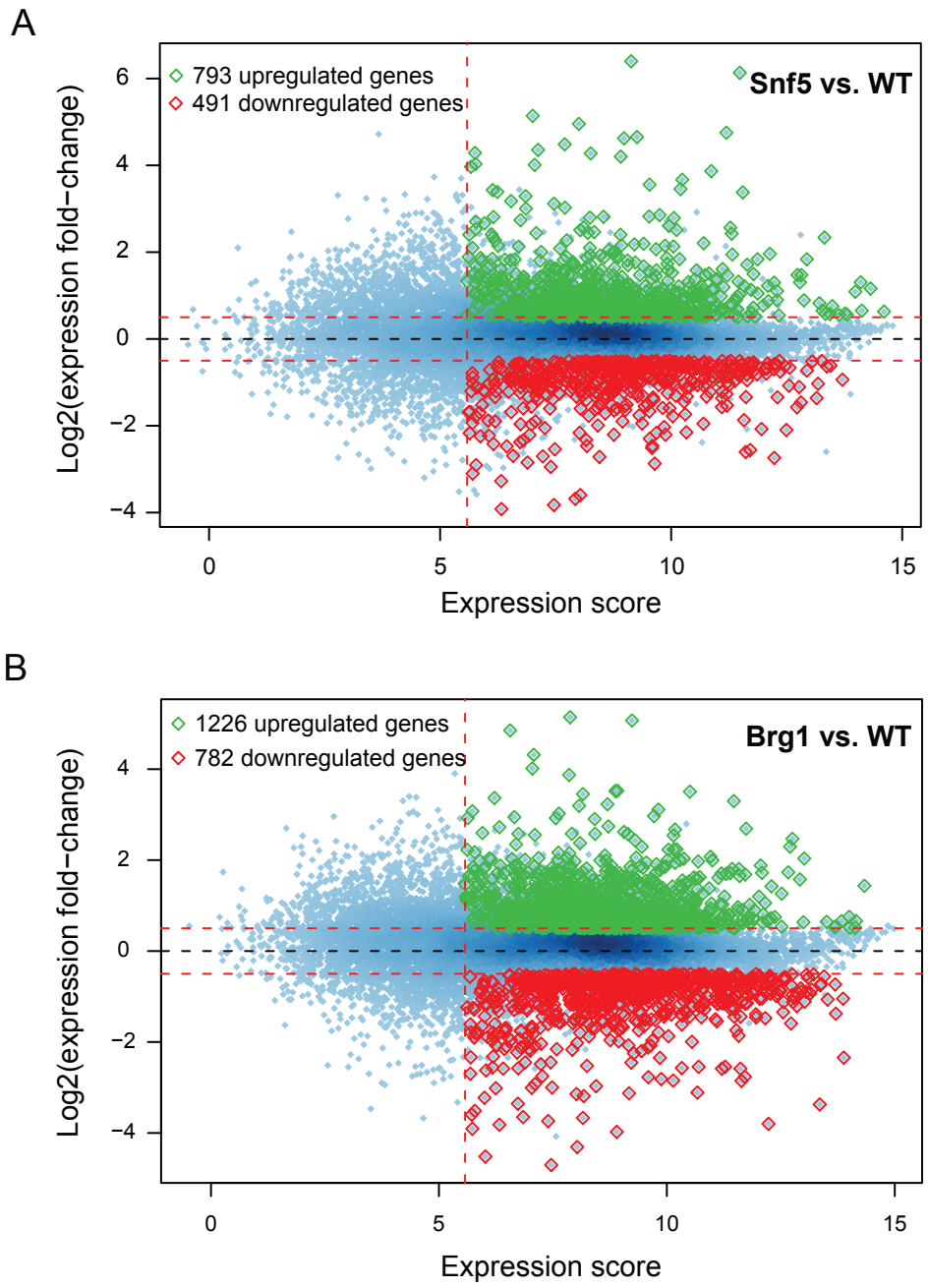

Figure S6. Gene expression changes following inactivation of Snf5 and Brg1. *(A)* Comparison of the gene expression in Snf5-deficient and WT cells. Each point represents a gene interrogated on the microarray. The x-axis indicates magnitude of expression (the greater of WT or Snf5-deficient) and the y-axis (log2 scale) indicates fold-change in expression. Up- and down-regulated genes (green and red diamonds) were identified as those with the expression level and change above thresholds (shown with dashed red lines) and with the p-value for expression change below 0.05 (see Methods for details).
(B) The same as *(A)* for Brg1 depleted cells.

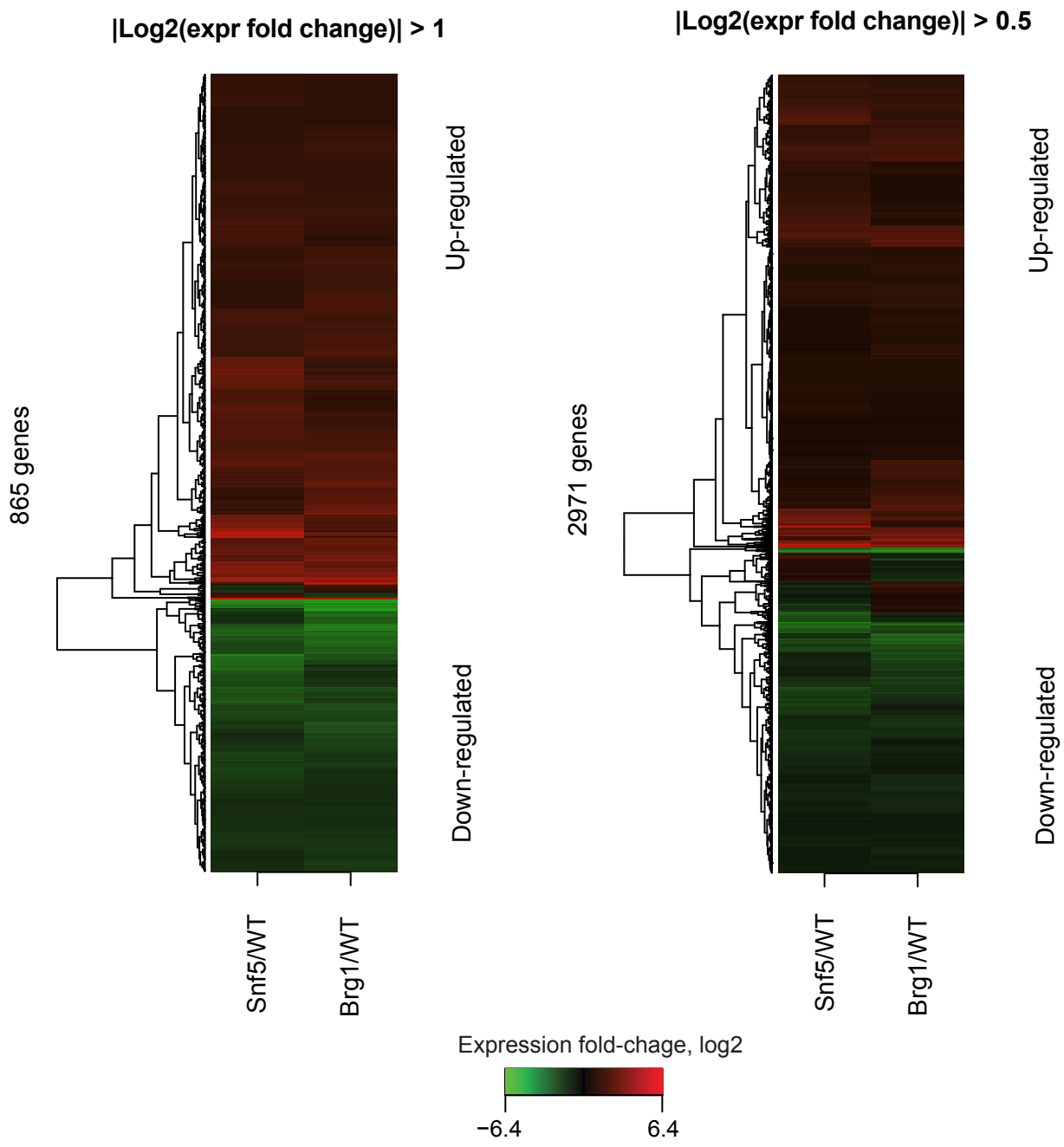

Figure S7. Hierarchical clustering of the genes based on expression fold changes upon Snf5 or Brg1 inactivation. Each panel corresponds to the sets of genes with expression fold changes above the specified threshold. Note that most genes are co-regulated in both mutant samples.

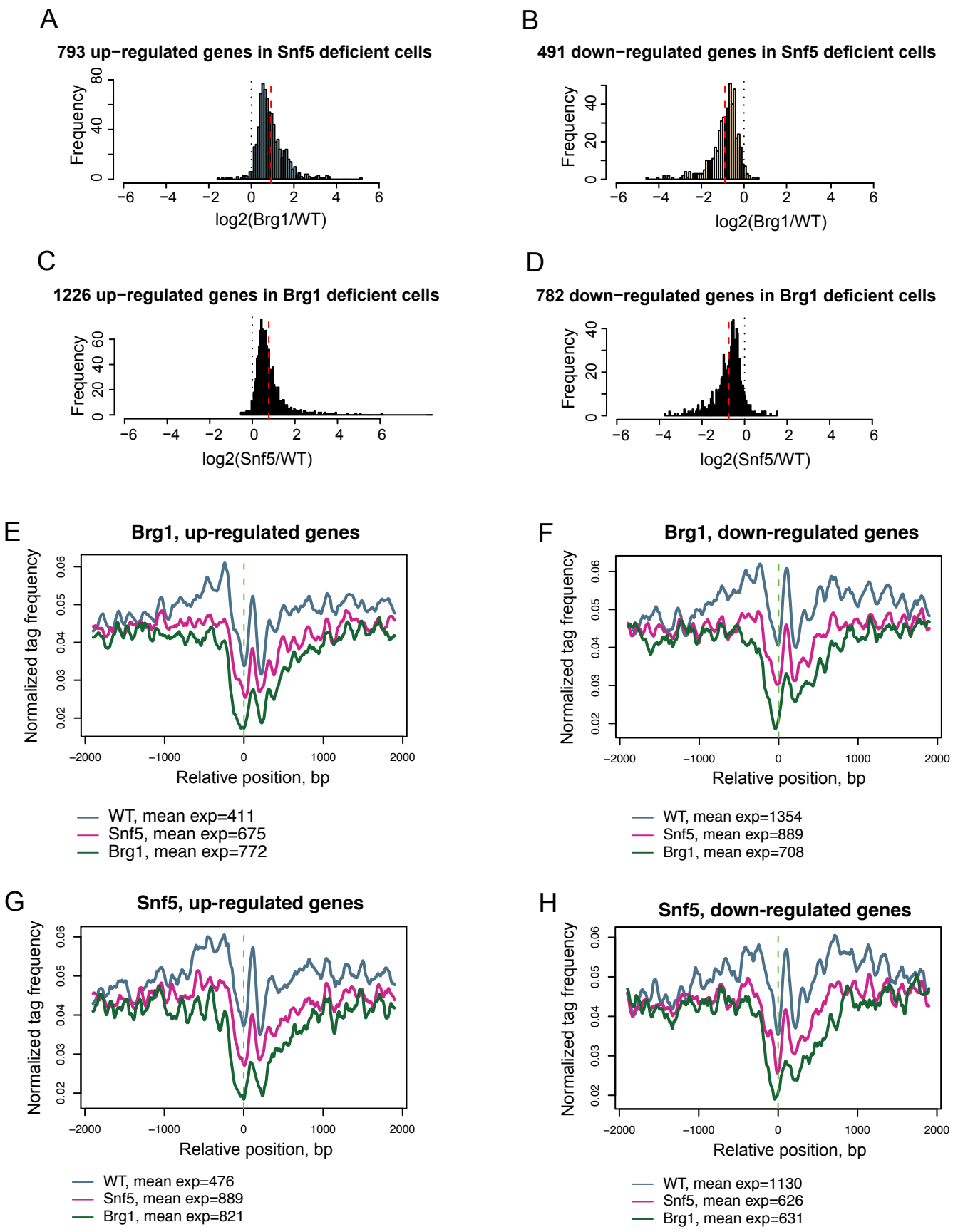

Figure S8. Loss of Brg1 or Snf5 has similar effects on nucleosome occupancy and gene expression. (*A, B*) Histograms showing the effects on gene expression induced by Brg1 deletion for genes that were up-regulated (*A*) or down-regulated (*B*) in Snf5 deficient cells. (*C, D*) Analogous analysis for the genes identified as up- and down-regulated in Brg1 deficient cells.
(*E-H*) Nucleosome occupancy profiles for the genes up- and down-regulated upon inactivation of either Brg1 (*E,F*) or Snf5 (*G,H*). The mean expression values are provided for each gene group below the plots.

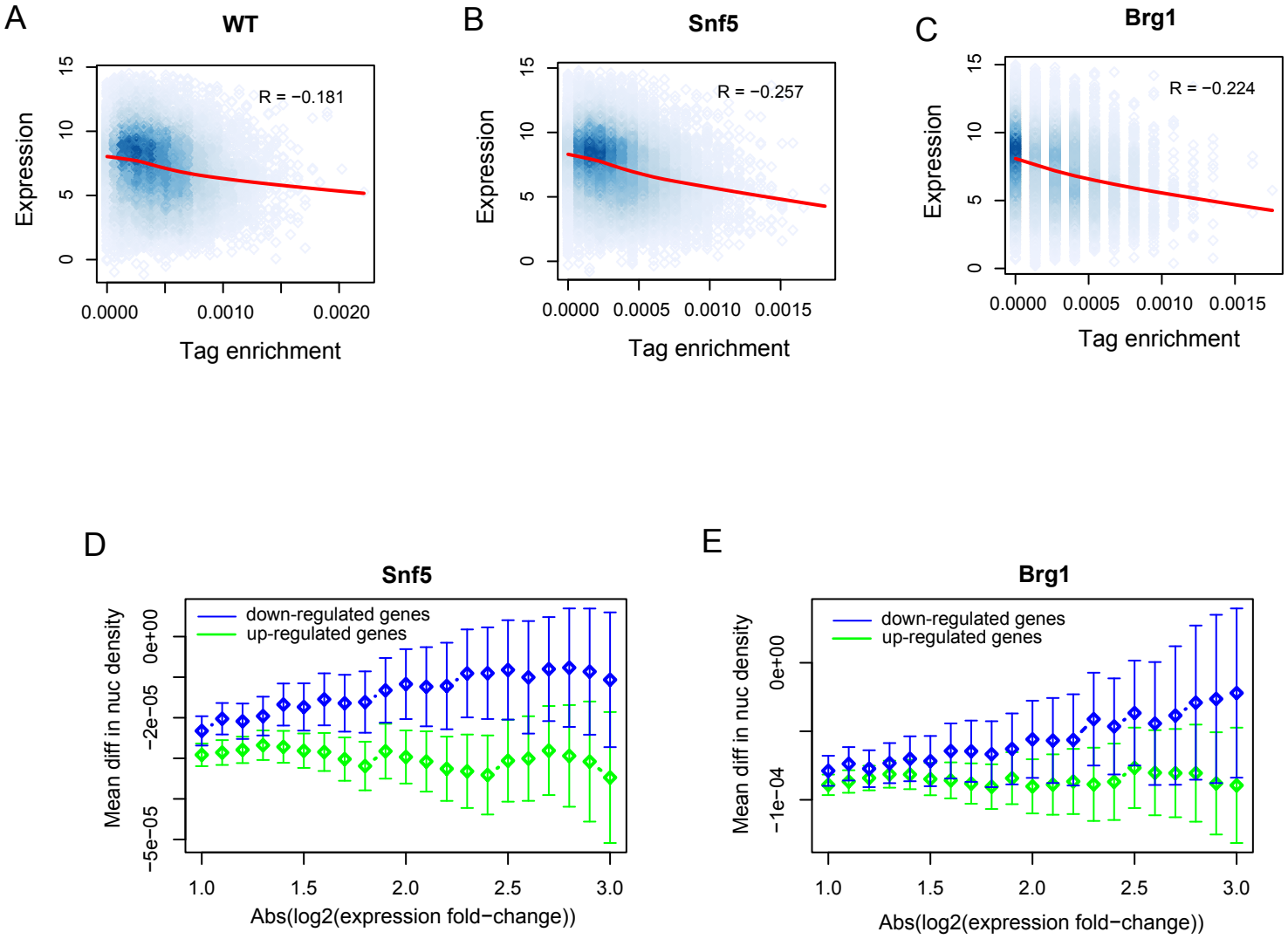

Figure S9. Relationship between nucleosome occupancy and gene expression.
(A-C) Gene expression compared to nucleosome occupancy at the NDR in WT, Snf5-deficient, and Brg1-deficient cells respectively. Each dot on the plots represents a gene and the red lines represent loess regression lines. Pearson correlation coefficients are shown inside the plots.
(D,E) Dependence of gene expression fold-change on the difference in nucleosome occupancy in Snf5- and Brg1-deficient cells. Up-regulated (green) and down-regulated (blue) genes were grouped according to their expression fold-changes as compared to WT (absolute values of log2 of the expression fold-changes were used). Then, the mean differences in the nucleosome tag density in the regions +/-2 kb around genes in WT and mutant cells were calculated for each gene group separately. The 95% confidence intervals are also shown for each group.

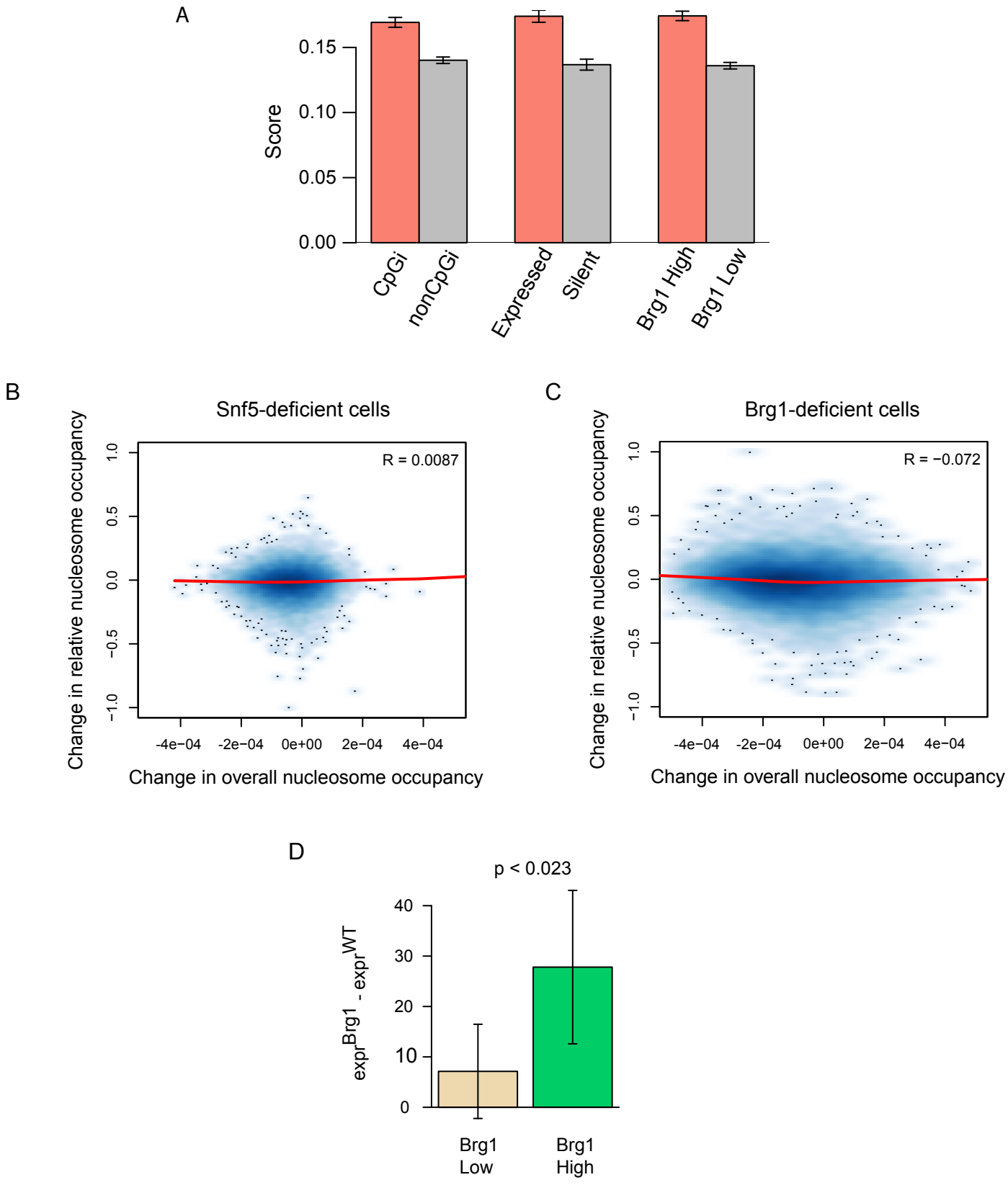

Figure S10. Relation between different features of chromatin remodeling and transcription.
(*A*) Relationship between relative occupancy score and CpGi presence, expression status, and Brg1 enrichment at TSS in WT sample. *(B,C)* Absence of correlation between changes in overall nucleosome occupancy at TSS and relative occupancy score in Snf5- and Brg1-deficient samples. *(D)* Genes with higher levels of Brg1 enrichment are associated with stronger changes in gene expression upon Brg1 inactivation. Mean changes in expression upon Brg1 inactivation are compared for the genes with low and high Brg1 enrichment (yellow and green bars respectively). The 95% confidence intervals and p-value of difference are shown.